

## FE assessment of dissipative devices for the blast mitigation of glazing façades supported by prestressed cables

Claudio Amadio<sup>a</sup> and Chiara Bedon\*

*Department of Engineering and Architecture, University of Trieste, Piazzale Europa 1, 34127 Italy*

*(Received April 20, 2011, Revised May 15, 2014, Accepted May 18, 2014)*

**Abstract.** The paper focuses on the dynamic response of a blast-invested glass-steel curtain wall supported by single-way pretensioned cables. In order to mitigate the critical components of the façade from severe structural damage, an innovative system able to absorb and dissipate part of the blast-induced stresses in the critical façade components is proposed. To improve the blast reliability of the studied glazing system, specifically, rigid-plastic and elastoplastic devices are introduced at the base and at the top of the vertical bearing cables. Several combinations and mechanical calibrations of these devices are numerically investigated and the most structurally and economically advantageous solution is identified. In conclusion, a simple analytical formulation totally derived from energetic considerations is also suggested for a preliminary estimation of the maximum dynamic effects in single-way cable-supported façades subjected to high-level blast loads.

**Keywords:** single-way cable-supported façade; explosions; dissipative devices; energy approach; nonlinear dynamic simulations

---

### 1. Introduction

During the last decades, an increasing number of buildings have been coated by means of glazing curtain walls. This technological choice, generally associated to primarily architectural and esthetic aspects, currently represents for structural engineers a widespread topic in continuous development.

In this context, numerous authors investigated the behavioral trends of these innovative structural systems, focusing on several aspects and specific loading / boundary conditions (Feng *et al.* 2009, Li *et al.* 2005, Schlaich *et al.* 2005, Weggel *et al.* 2007). Recently, the effects of possible explosive events in the response of such slight systems have also been taken into account and assessed by means of finite-element (FE) numerical investigations, experiments and analytical studies. The design approach for glazing surfaces able to resist explosions ('*Blast resistant glazing façades*') is in fact markedly different from the design requirements of buildings subjected to ordinary loads (Baker *et al.* 1983, Norville and Conrath 2001, Schmidt *et al.* 2003).

Firstly, the basic prerequisite of structural systems subjected to explosive loads is the

---

\*Corresponding author, Post-Doc. Researcher, E-mail: [bedon@dicar.units.it](mailto:bedon@dicar.units.it)

<sup>a</sup>Professor

minimization of possible injuries. Explosive loads represent extreme, accidental events characterized by abrupt release of energy, typically associated to high intensity and short duration, therefore certain level of damage in the involved buildings is generally accepted. Secondly, it should be noticed that engineers are often committed to design glazing façades able to remain sealed after the explosion has been occurred, hence resulting in curtain walls able to prevent the penetration of the shock wave into the buildings. Undoubtedly, it is clear that this design strategy allows not only to reduce the damage that may occur on the occupants, but also to preserve the activities within the buildings once the explosion has been occurred (Corely *et al.* 1998, Mays and Smith 1995, Norville *et al.* 1999, Smith 2001).

To achieve these important objectives, the bearing structure (e.g., the structural background and the supporting frame or bracing system) as well as the fixing components of the façade should be essentially able to resist the design blast load. At the same time, the coating should be sufficiently resistant and flexible, so that it could dissipate as much energy as possible. Over the last decades, various technological and manufacturing improvements provided continuous and innovative support to façade designers. Laminated glass, for example, in which two or more glass panels are connected together by means of thermoplastic foils able to provide a certain level of structural interaction between them (PVB, for example) represented for a long period the typical “blast resistant glass”. The main advantage of laminated glass elements is in fact primarily given by the lack of detachment of glass shards and fragments, once the glass panels are cracked. At the same time, due to the intrinsic plasticity provided by the adopted interlayers to typically brittle-elastic glass panels, laminated glass elements can partly dissipate the incoming energy due to impact loads such as explosions. Nevertheless, especially under extreme loading conditions, laminated glass alone cannot provide enough post-cracked residual strength and appropriate damping capabilities to complex glazing systems, and the required levels of structural dynamic performances could be obtained only by means of additional dissipative components.

In a glazing façade sustained by pretensioned cables, for example, both the glass panels and the cables are typically designed so that they could resist to ordinary wind loads. The optimal design solution should be detected - based on structural, economical and feasibility considerations - so that the thickness of glass sheets (e.g., the total mass of the façade) and the diameter / pretension level in the cables could offer limited deflections (e.g., 1/40 the total span) under wind pressures. In presence of high-level impulsive loads such as explosions, in this context, the use of opportune devices able to partly dissipate the incoming energy transmitted by the shock wave could improve the global response of these curtain walls. Such devices could be introduced, for example, where the bearing cables are directly connected to the main structure. In this manner, the high-rate pressure forces affecting the glass panels would not be completely transformed into elastic energy deforming the cables but a part of the incoming energy could be dissipated by the proposed devices.

In the paper, the dynamic behavior of a cable-supported façade subjected to high-level blast loads is investigated numerically and analytically. In order to individuate the critical components of the blast-invested façade and to assess the structural efficacy of the proposed devices - e.g., in terms of stresses and displacements mitigation in the façade components - a sophisticated FE model is presented. Three possible solutions are presented, which respectively foresee the use of a single vertical device introduced (i) at the top or at the base of each cable, as well as the combined use of two devices ((ii) vertically or (iii) horizontally oriented, respectively), introduced at both the ends of the pretensioned cables. Based on a wide series of parametric nonlinear dynamic analyses, the most efficient solution is identified. Finally, a simple analytical formulation is also presented

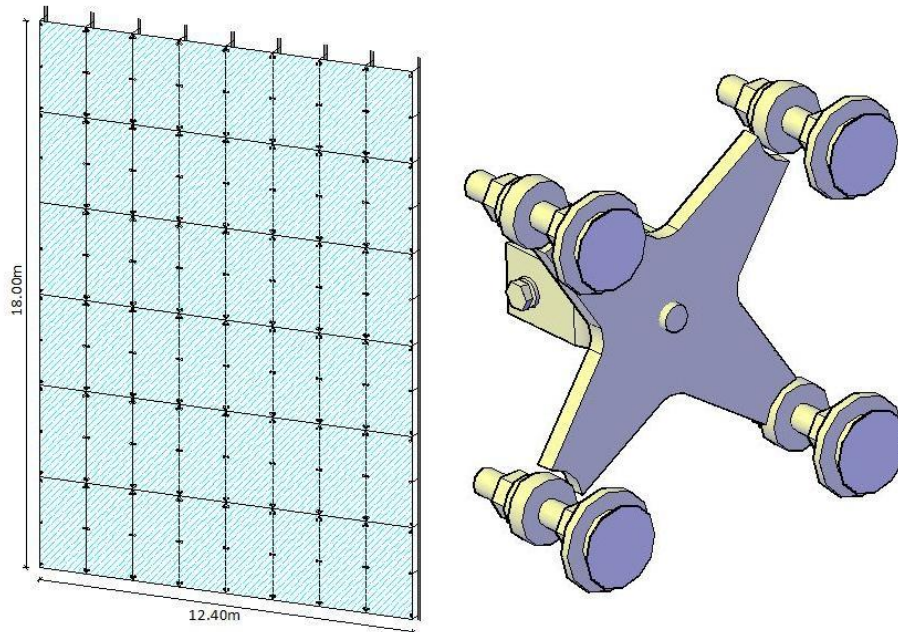


Fig. 1 Elevation of the cable-supported façade and example of a four-hole spider connector

for an approximate and rational estimation of the maximum effects due to a given explosive load on single-way cable-supported façades.

## 2. Independent cable-supported glazing façades

An independent cable-supported glazing façade consists in three basic components: the glass panels, the pretensioned cables and special connectors able to provide a certain structural interaction between the glass panels and the cables (Lam *et al.* 2004). In order to obtain a weather-tight curtain wall and to bond together the glass panels, the space between them is typically filled with structural silicone sealants. The main role of the pretensioned steel cables consists in supporting the glass panels and in transferring the orthogonal loads (e.g., wind pressures) to the foundation or to other bearing structures (e.g. structural background).

Special connectors, in this context, allow the realization of a cable-glass system in which the glass panels work together with the pretensioned cables. ‘Spider devices’, for example, represent a point-fixed joint typology largely used in suspended façades. They typically consist of a stainless steel four-hole cross-bar linked to the glass panels through fasteners (e.g., *rotules*) clamped at the corners of the glass sheets. Each cross-bar is then connected to the adjacent pretensioned cable through a stainless steel bar (Fig. 1, detail). Additional point supports are generally introduced also at the mid-span vertical edges of the glass elements, in the form of two-hole connectors, so that each panel could result six-point supported. The studied façade is  $L=18.00$  m long and  $B=12.40$  m wide, and consists in laminated glass sheets of nominal dimensions  $b=1.55$  m  $\times$   $h=3.00$  m (Fig. 1). Each laminated glass panel has a total thickness  $t=24.5$  mm, obtained by assembling two tempered glass elements ( $t_1=t_2=10$  mm) and a middle PVB interlayer ( $t_{PVB}=4.5$  mm). The vertical steel cables

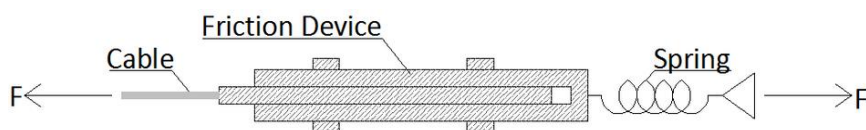


Fig. 2 Dissipative device (cross section)

have diameter  $\phi=36$  mm and are subjected to an initial pretension force  $H_0=370$  kN. To form a bearing system, they are 1.55 m-spaced along the width of the façade. In the direction perpendicular to the plane of the façade, conversely, the distance between the cables and the glass panels is  $d_c=65$  mm. Each glass sheet is six-point supported and joined together at the cables by means of stainless steel spider devices.

### 2.1 Elastoplastic devices

An elastoplastic device can be considered composed of two components working in series (Fig. 2), namely:

- a simple rigid-plastic friction apparatus, able to partly dissipate the incoming energy through the sliding of two metallic surfaces in contact, and
- an elastic axial spring, able to provide additional elastic deformations to the device itself.

Three metallic plates (e.g., made up of stainless steel or brass), joined together by a series of pretensioned bolts, and a slotted hole, can be properly assembled to obtain a functional friction mechanism. While the two outer plates are directly connected to the bearing structure, the middle plate is connected to the pretensioned cable. As a result, the main parameter able to describe the rigid-plastic behavior of the friction mechanism is the sliding force  $F_{y,D}$ . As far as the maximum axial force in the single cable exceeds the sliding force  $F_{y,D}$ , the frictional mechanism is activated. Otherwise, the frictional device does not slide and provides a perfectly rigid connection to the cable, hence resulting in a cable-supported façade rigidly connected to the structural background.

At the same time, the linear elastic component of the dissipative device can be described in the form of a spring, whose mechanical performance is typically defined by the elastic stiffness  $k_{device}$ . A proper mechanical calibration of the frictional and elastic component, as shown in the following sections, could provide a marked improvement in the dynamic capabilities of the cable-supported façades, hence resulting in significant mitigation of its components.

### 2.2 Blast wave front definition

In order to simulate the blast wave pressure and its effects on the studied façade, a self-made computer software was used. The computer program defines the pressure function versus the time, plotted in two phases. The positive pressure phase is defined by the exponential equation proposed by Friedlander (Bulson 1997)

$$p(t) = p_0 \left( 1 - \frac{t}{t_d^+} \right) e^{-k_p \frac{t}{t_d^+}}, \quad 0 \leq t \leq t_d^+ \quad (1)$$

Eq. (1) fits the pressure waveform between the instant zero of maximum overpressure  $p_0$  and the instant  $t_d^+$  at the end of the positive phase. The overpressure  $p(t)$  strictly depends on three main

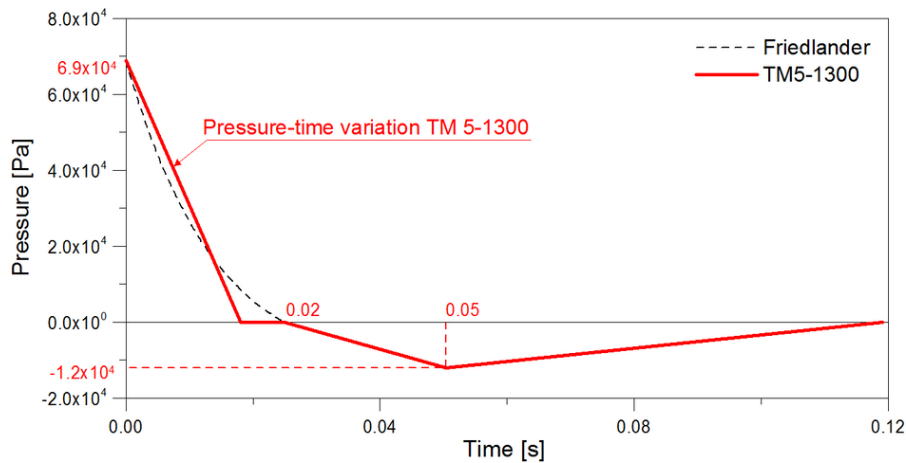


Fig. 3 Time-varying pressure function representative of a Level D-GSA blast load

parameters and specifically (i) the distance between the explosion source and the invested building (*stand-off distance*), (ii) the height of the explosion source from ground and (iii) the quantity of detonating explosive (*equivalent mass* of TNT). The computer program defines the static overpressure peak  $p_0$  characterizing the blast wave front in accordance with the recommendations of the TM 5-1300 standards (1990). The shape coefficient  $k_p$ , representative of the velocity of decay of the overpressure peak  $p_0$ , is automatically calculated by the numerical code. Finally, the negative phase of the time-varying pressure wave is schematized in the form of a triangular shape, as proposed by the reference US Code.

In the specific circumstance, the considered high-level blast load is classified as “Level D” (GSA-TSO1-2003). The main outputs of the software are the impulse per unit of surface ( $i=613.7$  kPa·ms), the static overpressure peak ( $p_0=69.9$  kPa), the maximum duration of the positive phase ( $t_d^+ = 0.02$  s), as well as the corresponding time-varying pressure function (Fig. 3).

### 2.3 FE modeling of the façade

Incremental numerical analyses partly discussed in the paper have been performed by means of sophisticated FE models carried-out by using the computer software ABAQUS (Dassault Systèmes Simulia Corp. 2009). Since the examined façade was sufficiently wide ( $B=12.40$ m, Fig.1) to consider negligible the effects of possible lateral restraints, the minimum dimension of a single laminated glass panel was taken into account and a single, geometrically simplified façade-module was analyzed. The typical FE model, in these hypotheses, consisted of six glass sheets arranged along the height of the façade, a pair of pretensioned cables and a series of half-spider devices, hence resulting in a modular-unit 1.55m large and 18.00m tall (Fig. 4). In order to avoid high computational cost of nonlinear dynamic simulations, as explained in the latter, this modeling assumption was taken into account together with appropriate restraint conditions.

The laminated glass panels were modeled in the form of three-dimensional, four-node multi-layer shell elements (S43, *composite shell*), able to properly simulate membrane behaviors also under high-strain dynamic loads. This modeling choice allowed to take into account the effective nominal thickness of the laminated glass cross-section (e.g., the glass panels and PVB-film), as

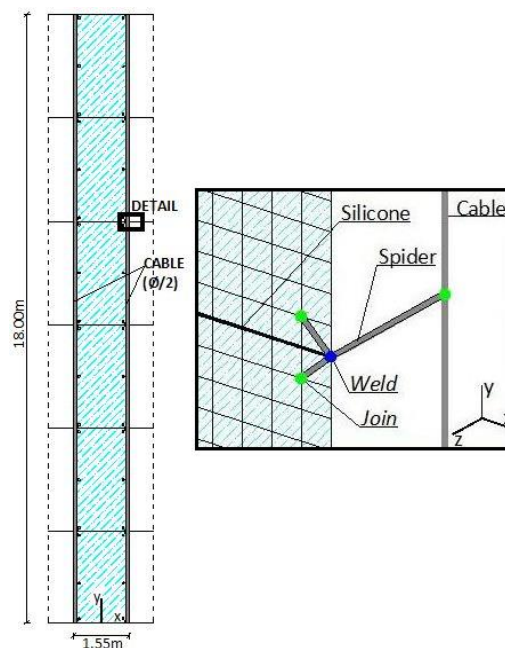


Fig. 4 Front view of the studied FE-façade-module and detail of a half-spider connector

well as to preserve the computational cost of analyses, compared for example to full solid FE-models.

Meshing of the model was based on 200mm square module, both for the glass panels and the cables. As a result, glass elements were described by means of a regular 200mm x 200mm pattern. The glass panels were allowed to oscillate in the  $z$  direction only, so that in the investigated façade-module could be properly taken into account, when subjected to the design blast load, the presence of adjacent glass panels. For this purpose, both the  $u_x$  and  $u_y$  displacements of glass mesh nodes, as well as their  $r_y$  and  $r_z$  rotations, were restrained.

The pretensioned cables were then modeled as *truss* elements (T3D2), characterized by a cross-sectional area equal to half the nominal one, due to the basic assumptions of the single façade modular unit. In doing so, the cables were pinned at the upper end, and the initial pretension force was applied by imposing an equivalent vertical displacement at their base. Along the height of the façade-module, only the  $u_z$  displacements and the  $r_x$  rotations were allowed for the cable nodes.

Appropriate modeling assumptions were then taken into account to properly describe the structural interaction between the glass panels and the supporting cables.

Concerning the cable-glass joints, specifically each spider device was modeled in the form of three rigidly connected beams (B31). These beams were linked together through a *weld* connector. At the same time, the spider components were respectively connected to the cables and to the laminated glass panels by means of *join* connectors able to allow them to freely rotate (Fig. 4, detail). At the same time, the structural silicone sealant bonding together the glass panels was introduced in the investigated façade-module in the form of *slot + euler* connectors. As a result, the silicone sealant foils consisted in a series of equivalent springs acting in the same plane of the glass panels ( $k_{silicone}=1.67 \times 10^5$  N/m).

Careful consideration was then paid for the mechanical calibration of materials (Table 1). In

Table 1 Mechanical properties of materials

Material	Density [kg/m <sup>3</sup> ]	Modulus of elasticity [N/m <sup>2</sup> ]	Poisson's ratio	Behavior [-]
Glass	2490	7x10 <sup>10</sup>	0.23	Linear elastic
PVB	660	5x10 <sup>8</sup>	0.50	Elastoplastic
Harmonic steel (cables)	7300	1.3x10 <sup>11</sup>	0.32	Linear elastic
Stainless steel (spider devices)	7300	2.1x10 <sup>11</sup>	0.32	Linear elastic

cable-supported façades, the failure of glass panels should be avoided, being their integrity fundamental to preserve the stability of the entire curtain walls. In these hypotheses, glass was preliminarily described in the form of an isotropic, indefinitely linear elastic material, having nominal Young's modulus, Poisson's ratio and density collected in Table 1. For the PVB-film, at the same time, an elastoplastic characteristic curve was taken into account (with  $\sigma_{y,PVB}=8$  MPa the failure strength), since able to properly simulate the mechanical behavior of PVB foils under high-strain impulsive loads. Steel composing the cables and the point-connector, finally, was described as a linear elastic material (Table 1).

In order to describe realistically the effects of the design explosion on the dynamic response of the studied façade, all the numerical analyses were performed by taking into account possible damping effects, although generally negligible. A total damping ratio  $\zeta_{TOT} \cong 3.2\%$  was used, being estimated as the sum of structural, aerolastic and PVB-material damping terms (Feng *et al.* 2009). This contribution was then described in the form of a Rayleigh mass proportional damping.

A distributed pressure, acting in the direction perpendicular to laminated glass panels was finally taken into account to be described, in accordance with the time-varying pressure function proposed in Fig.3, the blast load affecting the investigated façade-module.

### 3. Dynamic analyses for the façade not equipped by dissipative devices

#### 3.1 Modal analysis

Cable-supported façades subjected to blast loads typically behave geometrically nonlinearly and the first vibration mode is representative of their predominant deformed shape. By using the FE model previously described, a linear modal analysis was preliminarily performed on the studied façade-module and three vibration modes were predicted. In doing so, only the initial pretension force  $H_0=370$  kN was considered affecting the bearing cables, and they were assumed to be rigidly connected at the ends (e.g., no friction devices). The fundamental period of vibration of the façade-module resulted equal to  $T_0^{FE} = 0.51$ s, being the first modal shape characterized by a sine-shaped deformed configuration.

#### 3.2 Incremental nonlinear analyses

The dynamic response of the façade-module not equipped by the proposed dissipative devices was successively investigated in presence of several blast load distributions. The aim of this preliminary numerical simulation phase consisted in the assessment of possible effects due to the negative phase of blast (Fig. 3). Consequently, two load cases were taken into account:

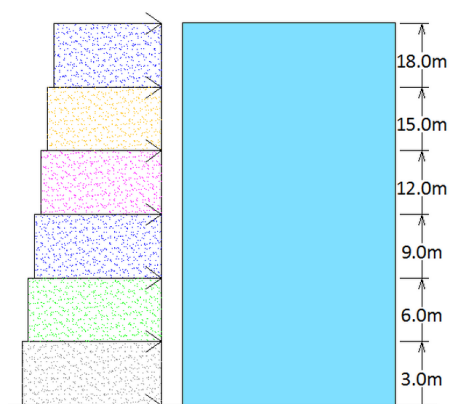


Fig. 5 Simplified distribution of the blast wave front along the elevation of the façade-module

- LC-1: Level D-GSA blast load, characterized by the positive phase only;
- LC-2: Level D-GSA blast load, described in the form of both the positive and negative phases.

A set of time-varying pressure functions were defined with the same numerical code previously described, since the overpressure peak and the time of impact characterizing the generic blast wave front - and therefore the corresponding impulse - is a function of the distance from ground of the impacting surface.

Based on the nominal  $b \times h$  dimensions of each laminated glass panel, six pre-established levels were considered along the elevation of the façade-module (0.0 m, 3.0 m, 6.0 m, 9.0 m, 12.0 m, 15.0 m). The obtained blast wave pressures were subsequently introduced in the FE model in the form of uniformly distributed-time varying pressures, acting orthogonally to the plane of the curtain wall. In this manner, the façade-module globally resulted affected to six constant overpressure parts (Fig. 5).

All the dynamic numerical analyses discussed in this paper consisted in two separate steps. Firstly, the initial pretension force was introduced in the bearing cables ( $0 \leq t \leq 0.10$ s). Successively ( $t \geq 0.10$ s), the design blast load was also taken into account. The typical dynamic response of the investigated façade-module is proposed in Fig. 6.

In the figure, a sequence of maximum tensile stresses occurring on the glass surface is shown, as a function of time. The proposed contour plots, referred each one to a specific instant of the analysis ( $t=0.12$ s, 0.15s, 0.18s and 0.20s, respectively), qualitatively emphasize the distribution of tensile stresses in the glass panels immediately after the explosion.

The glass panes, as shown, are certainly the most critical component of the entire suspended curtain wall, since they present a brittle behavior and they are subjected to significant flexural strains, being the first component of the glazing system affected by the incoming pressures. Therefore, it is important to avoid the attainment in the glass sheets of tensile stresses exceeding the material design strength, since this event would induce considerable damages to the stability of the entire façade and to the occupants of the building.

As shown in Fig. 6, the distribution of the maximum tensile stresses rapidly modifies in time. Initially, maximum peaks of tensile stress are attained near the restraints of the façade-module (Fig. 6,  $t=0.12$ s and  $t=0.15$ s). Subsequently, maximum stresses gradually transfer towards the center of the façade-module, until the glass panels release a significant part of the stored kinetic energy due to the explosive event (Fig. 6,  $t=0.18$ s and  $t=0.20$ s).

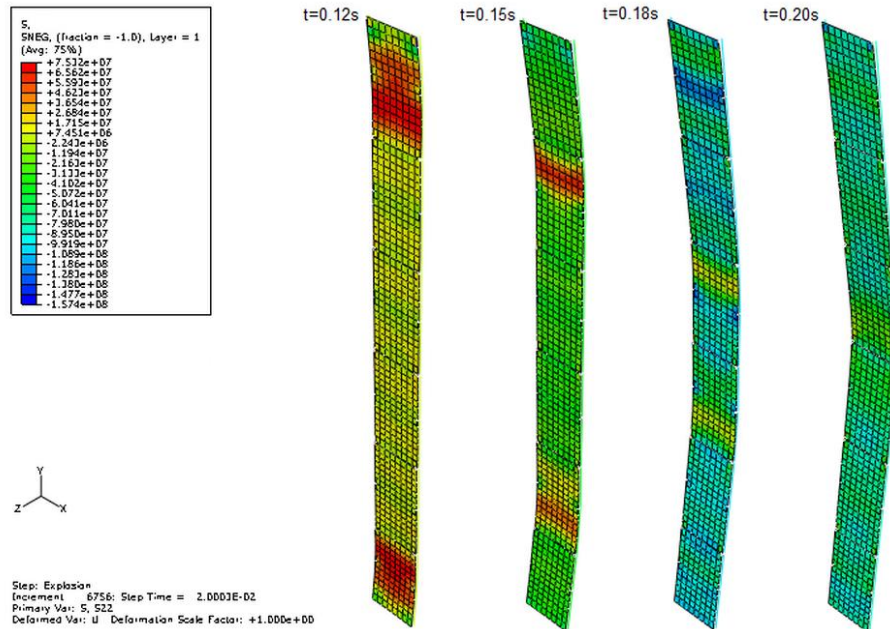


Fig. 6 Sequence of distribution of maximum tensile stresses on glass surface, as a function of time

A typical property of glass curtain walls supported by pretensioned cables is that the blast-involved effects do not simultaneously affect the entire façade. The blast wave front acts in fact as a moving load, firstly interesting the most rigid zones of the curtain wall (e.g., the edges near the top and bottom end restraints) and subsequently moving towards its center. Moreover, the amount of these tensile stresses is generally proportional to the rigidity of the restraints, as expected. It is consequently clear that the maximum stresses achieved in presence of bracing cables able to gradually absorb the blast-incoming energy would be unavoidably lower than the stresses attained in presence of a rigid bearing structure (e.g., a frame).

Just because of these reasons, it is possible to perceive that the pretensioned cables offer significant advantages in the design of blast resistant glazing façades, due to their intrinsic shock absorbing property and to the particular way they deform, preventing the attainment of dangerous peaks of stresses in correspondence of the fixing connectors. On the other hand, it cannot be neglected that this typology of glazing façades still represents a rather sophisticated technological solution, since the cables are subjected to high tensile stresses and possible glass fragments could be thrown out at high velocities. At the same time, it should be mentioned that the design of similar blast-resisting system should provide an optimal balance between structural, economical and feasibility aspects, hence resulting in complex procedures.

The performed numerical analyses allowed to notice that for the examined façade-module, for example, maximum displacements are approximately attained at the instant  $t \cong 0.20s$ .

The maximum velocity of the moving façade-module during the explosive event, representative of the speed of possible glass fragments thrown out after the façade breakage, is approximately equal to  $\dot{u}_{\max} \cong 15m/s$ .

In correspondence of the maximum deformed configuration, high peaks of tensile stresses affect the mid-span laminated glass panel (Fig. 7). Furthermore, the blast wave front exclusively

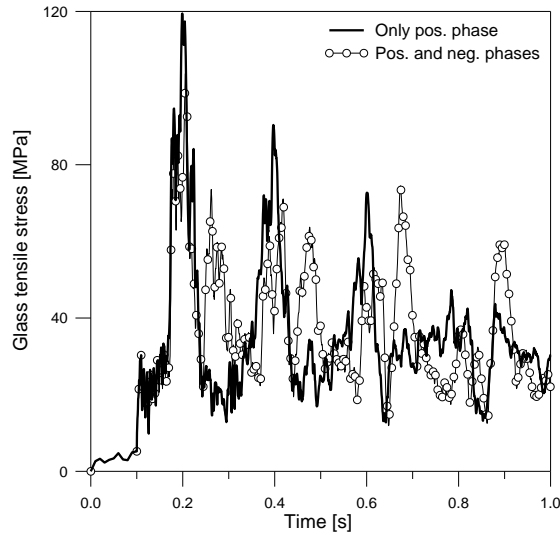


Fig. 7 Envelope of maximum tensile stresses in the mid-span glass panel, as a function of time

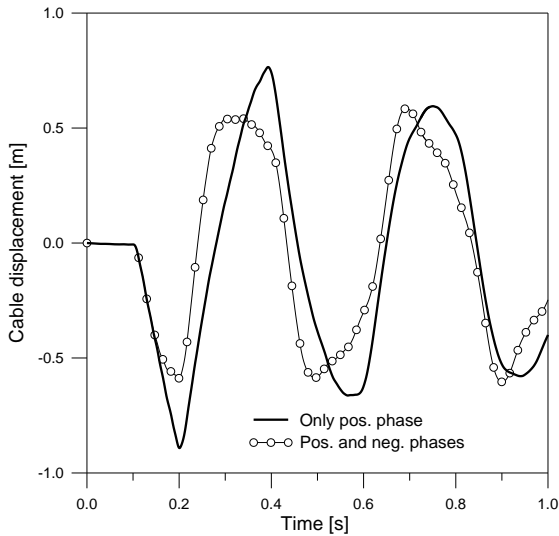


Fig. 8 Displacement of the cables, as a function of time

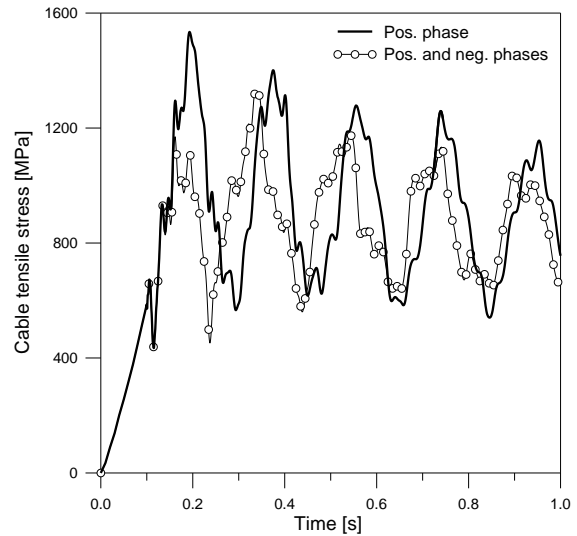


Fig. 9 Tensile stresses in the cables, as a function of time

defined in terms of positive phase – as expected – involves most serious tensile stresses in the central glass sheet, not only in the instant of maximum deflection ( $\sigma_{glass,max}^{pos} \cong 119\text{MPa}$  and  $\sigma_{glass,max}^{pos,neg} \cong 104\text{MPa}$ , Fig. 7), but also in the subsequent instants.

In the dynamic response of the blast-invested façade, also the pretensioned cables have an important role. The cables absorb not only the ordinary vertical loads but also the horizontal loads due to the blast wave front, therefore the axial forces to be taken up abruptly grows, until they attain a maximum peak ( $t \cong 0.20\text{s}$ ). In this specific circumstance, the blast-induced effects in the cables were investigated in terms of mid-span displacements (Fig. 8) and maximum tensile stresses

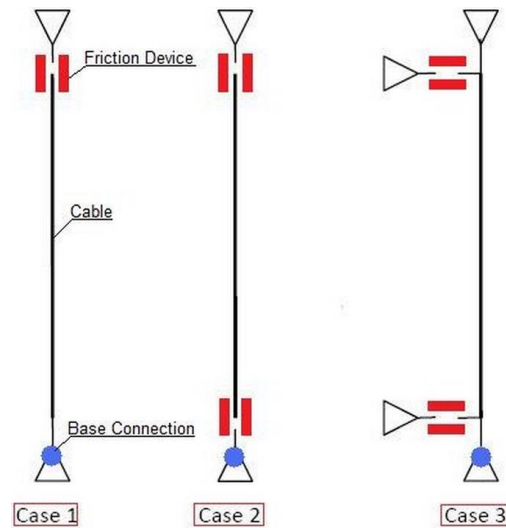


Fig. 10 Studied configurations for the façade-module equipped by elastoplastic devices

(Fig. 9). It is interesting to notice that considering the positive phase only or both the positive and negative phases for the examined Level D-GSA blast wave pressure, rather diverging maximum deflections ( $u_{cable,max}^{pos} \cong 0.9\text{m}$  and  $u_{cable,max}^{pos,neg} \cong 0.6\text{m}$ , Fig. 8), as well as maximum tensile stresses ( $\sigma_{cable,max}^{pos} \cong 1535\text{MPa}$  and  $\sigma_{cable,max}^{pos,neg} \cong 1170\text{MPa}$ , Fig. 9) were obtained. For this purpose, it cannot be ignored that the cables, composed of harmonic steel, presenting a typical elastic-brittle behavior characterized by high tensile resistance but almost null plastic deformations and residual strength before collapse. Consequently, when their cross section is not adequate to resist to the assigned blast loads, two main possible solutions are offered to designers in order to avoid an abrupt collapse of the entire suspended wall system. The first solution consists in increasing the cable diameter, while the second one consists in the introduction in the cable-supported façade of additional dissipative devices, able to mitigate possible structural damages by cutting down the blast effects and by improving the dissipative capabilities of the curtain wall.

#### 4. FE modeling of the façade equipped by dissipative devices

In a subsequent numerical investigation phase, the proposed dissipative devices were applied at the ends of the bearing pretensioned cables. Several solutions were taken into account and the FE façade-module was equipped by elastoplastic devices introduced at the top of the cables or at both their ends (Fig. 10). Specifically, three possible solutions are proposed in this paper:

- single vertical device: a single longitudinal device was applied at the top of each cable (Fig. 10, case 1);
- double vertical devices: double longitudinal devices were introduced at the top and at the bottom of each cable (Fig. 10, case 2);
- double horizontal devices: two devices, working orthogonally to the plane of the curtain wall (e.g., in the direction of the acting blast pressure) were applied at the top and at the bottom of each cable (Fig. 10, case 3).

In order to individuate the most appropriate technological solution, additional incremental dynamic analyses were performed. In doing so, the cable-supported façade-module equipped by dissipative devices was subjected to a Level D-GSA blast wave pressure defined in terms of its positive phase only (Fig. 3).

#### 4.1 Modeling of the dissipative device

The FE-model of the façade-module not equipped by devices was properly modified. Specifically, the friction component of the single dissipative device was modeled in the form of an *axial* connector, characterized by an opportune rigid-plastic behavior. Generally, the sliding force  $F_{y,D}$  of the purely friction component should be estimated by taking into account the effects of the pretension force, as well as additional static wind loads, and possible thermal excursions. In these hypotheses, based on preliminary considerations, a maximum sliding force  $F_{y,D,\max} = 750\text{kN} \cong 2.0H_0$  was considered when performing the incremental analyses on the FE façade-module equipped by single or double vertical devices (Fig. 10, *cases 1 and 2*, respectively), while the limit value  $F_{y,D,\max} = 80\text{kN} \cong 0.20H_0$  was taken into account for the third proposed solution (Fig. 10, *case 3*). The linear elastic spring working in series with the purely friction component of the dissipative device was also modeled in the form of an *axial* connector. Nevertheless, in the analyses partly discussed in this section, the elastic spring was preliminary assumed to behave rigidly ( $k_D = \infty \cong 1000 k_{\text{cable}}$ , with  $k_{\text{cable}}$  the axial rigidity of a single pretensioned cable), hence resulting in a perfectly rigid-plastic mechanisms able to interact with the cable-supported façade-module.

#### 4.2 Parametric dynamic nonlinear analyses

To individuate the most structurally and economically advantageous solution, the obtained parametric numerical results were compared with the dynamic response of the studied façade-module not equipped by dissipative devices.

Especially in terms of maximum displacements, negligible differences were generally noticed between the three examined solutions. The maximum deformed shape was in fact typically characterized by a mid-span displacement almost equal to  $u_{\text{cable},\max} \cong 0.94\text{m}$ , which approximately remained constant independently on the number or the mechanical properties of the used dissipative mechanisms (Fig. 11,  $t \cong 0.20\text{s}$ ).

Contrarily, the proposed devices clearly highlighted their beneficial contribution in terms of a marked reduction of the tensile stresses in the pretensioned cables (Fig. 12). In this context, it should be mentioned that undoubtedly, the presence of a sliding mechanism involves in the dynamic response of the façade a drop in the initial pretension force  $H_0$  affecting the cables, hence resulting in possible increase of maximum deflections. Another aspect that should be taken into account in the choice of the more appropriate solution, is that the total detensioning of the bearing cables - due to a possible extremely large sliding of the devices - could compromise the stability of the suspended curtain wall. As a result, proper calibration of each dissipative component should be generally provided.

Finally, the envelope of the maximum tensile stresses achieved on the surface of the mid-span laminated glass panel was also properly analyzed (Fig. 13). As a direct consequence of the almost negligible variation of maximum deflections in the cables, the beneficial role provided by the

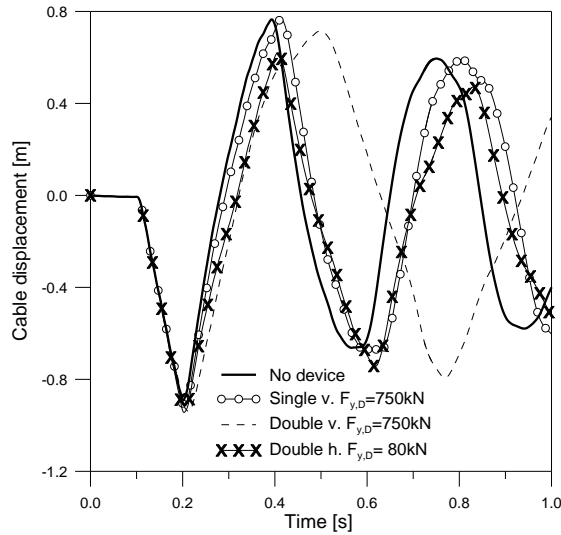


Fig. 11 Displacement of the cables (vertical or horizontal devices), as a function of time

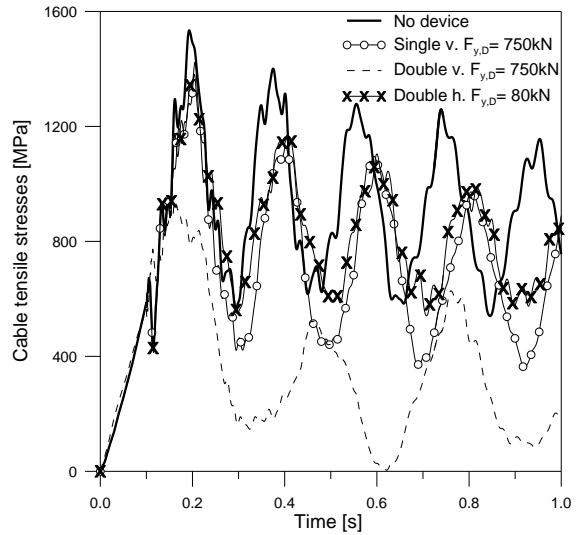


Fig. 12 Tensile stresses in the cables (vertical or horizontal devices), as a function of time

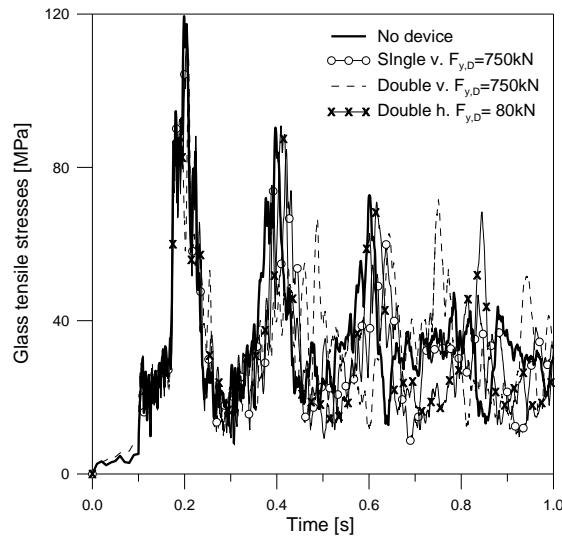


Fig. 13 Envelope of maximum tensile stresses in the mid-span glass panel (vertical or horizontal devices), as a function of time

single ( $\sigma_{glass,max} \cong 116\text{MPa}$ ), double vertical ( $\sigma_{glass,max} \cong 109\text{MPa}$ ) or double horizontal dissipative devices ( $\sigma_{glass,max} \cong 115\text{MPa}$ ) typically resulted negligible, compared to the façade not equipped by devices ( $\sigma_{glass,max} \cong 119\text{MPa}$ ).

#### 4.3 Choice of the optimal solution

Numerical simulations generally highlighted that the use of a single or double dissipative

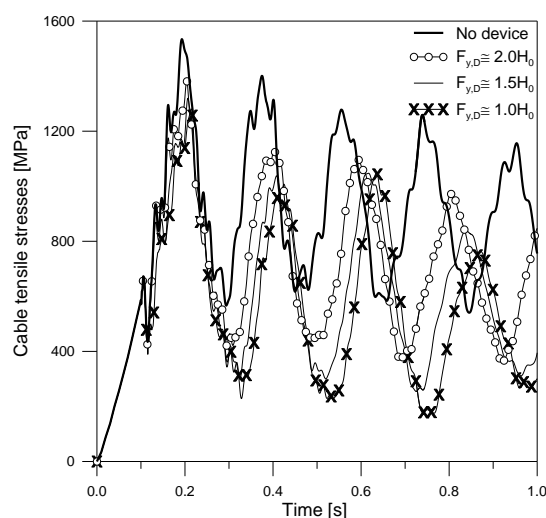


Fig. 14 Tensile stresses in the cables (single vertical device), as a function of time

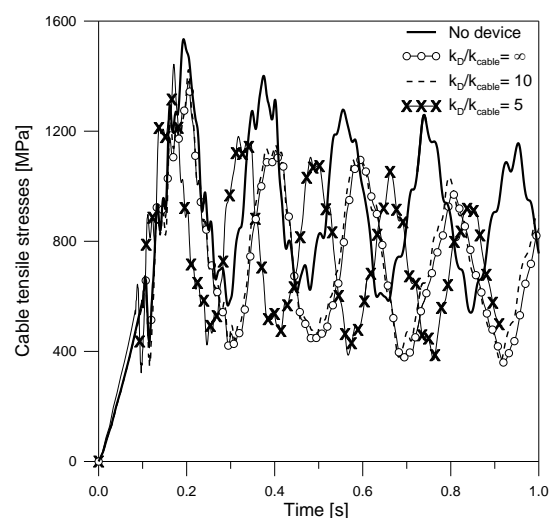


Fig. 15 Tensile stresses in the cables (single vertical device), as a function of time

device gives no marked advantages in terms of maximum displacements of the cables (Fig. 11), although the corresponding tensile stresses can be strongly reduced (Fig. 12). Furthermore, the presence of two vertical devices typically offered a more uniform decrease of the maximum axial forces in the bearing cables. On the other hand, although the performed analyses highlighted a large efficacy of double vertical devices, the observed structural benefits generally did not justify their double economic cost, compared to single devices only.

The third examined solution, foreseeing the use of two dissipative devices working in the direction perpendicular to the glazing surface, was proposed with the aim of controlling the sliding force  $F_{y,D}$  required for the activation of the dissipative mechanism. The introduction at the cables ends of a series of devices horizontally oriented, specifically, could allow the use of smaller devices, hence resulting in possible architectural advantages. In this context, further assessment of devices capabilities have been performed for the facade equipped by single dissipative mechanisms only.

#### 4.3.1 Effect of the sliding force $F_{y,D}$

The efficacy of a dissipative device characterized by a rigid-plastic behavior, as expected, is directly proportional to the amount of its sliding. For this purpose, an opportune estimation of the sliding force  $F_{y,D}$  is fundamental to properly control the maximum axial forces taken up by the bearing cables and the corresponding maximum deflections of the façade. To evaluate the effect of the sliding force  $F_{y,D}$  on the dynamic response of the blast-invested façade-module, further parametric analyses were performed by varying  $F_{y,D}$  in a pre-established range ( $1.0H_0 \leq F_{y,D} \leq 2.0H_0$ , with  $k_D = \infty \cong 1000 k_{cable}$ ). The obtained results were mainly analyzed in terms of maximum tensile stresses achieved in the pretensioned cables, since they constitute the main bearing component of the suspended curtain wall.

Generally, the sliding of the frictional device involves a marked reduction of the maximum tensile stresses in the pretensioned cables, as highlighted in Fig. 14. On the other hand, the sliding itself provides a drop in the initial pretension force that should be properly taken into account.

Especially in presence of limited sliding values  $F_{y,D}$ , the cables could be totally deprived of the initial pretension force, thus leading to a structural system not sustained by any bracing system. In order to optimize the benefits involved by frictional devices in the blast-induced response of the studied façade-module, the sliding force characterizing the behavior of the rigid-plastic dissipative mechanism should be set equal to  $F_{y,D} \cong 1.5H_0 - 2.0H_0$ .

#### 4.3.2 Effect of the elastic stiffness $k_D$

Additional numerical analyses were successively performed by changing the value  $k_D$  in a pre-established range ( $1 \leq k_D/k_{cable} \leq \infty$ ), in order to assess the possible effects of the elastic component on the overall behavior of the façade-module. The obtained mid-span displacements typically resulted only slightly increased by the combined elastic and plastic deformations of the dissipative mechanism ( $\Delta u_{\max} \cong 0.05\text{m}$ ). Independently on the amount of  $k_D$ , however, it should be noticed that the proposed dissipative devices provided marked decrease of the maximum stresses achieved in the bearing cables (Fig. 15).

In particular, the obtained tensile stresses generally resulted comprised between two limit conditions. The *upper limit* is typically associated to an extremely “rigid” dissipative device ( $k_D/k_{cable} \geq 30$ ) and is characterized by maximum values of tensile stresses which are not affected by the elastic component ( $\sigma_{cable,\max} \cong 1382\text{MPa}$ ; e.g., the behavior of the dissipative device is perfectly rigid-plastic). This limit condition should be avoided in the design of the dissipative mechanism, since the potentiality of the elastoplastic device could not be exploited at best. Contrarily, the *lower limit* condition ( $k_D/k_{cable} \leq 1$ ) represents the design condition in which the dissipative device does not plasticize.

The solutions comprised between these limit conditions are characterized by different amounts of elastic and plastic contributions of the dissipative devices. As displayed in Fig. 15, for example, the elastic spring constituting the proposed devices mainly highlights its benefits in the initial phase of the blast-induced dynamic response, that is in the instants in which the blast wave front abruptly affects the façade. Only in the subsequent instants, the friction component of the devices starts sliding and additional benefits can be achieved due to sliding of the metallic surfaces in contact.

## 5. Energy considerations

During the explosive event, the pressure forces exerted against the façade are not completely transformed into elastic energy deforming the steel cables, as generally happens in a façade not equipped by devices, but a part of this blast-induced increment of energy  $E_{blast} = \Delta E_0$  is dissipated or absorbed by the proposed devices. Specifically, during the initial part of the explosive event, the devices partly absorb the total increment of energy  $\Delta E_0$  due to the explosion

$$\Delta E_{device} = \Delta E_{friction} + \Delta E_{spring} \quad (2)$$

In Eq. (2)

$$\Delta E_{friction} = F_{y,D} s_{plastic} \quad (3)$$

is the blast energy term dissipated in heat by the sliding  $s_{plastic}$  of the purely friction mechanism. At

the same time

$$\Delta E_{spring} = \frac{1}{2} k_D \Delta z_{spring}^2 = \frac{1}{2} \frac{\Delta F_{spring}^2}{k_D} = \frac{1}{2} \frac{(F_{y,D} - H_0)^2}{k_D} \quad (4)$$

represents the increment of elastic energy stored by the spring constituting the dissipative device.

In Eq. (4), specifically:

-  $\Delta F_{spring}$  denotes the increment of force acting in the elastic axial spring at the examined instant. When the device attains its maximum deformed configuration,  $\Delta F_{spring} = F_{y,D} - H_0$ ;

-  $\Delta Z_{spring}$  is the lengthening of the spring due to  $\Delta F_{spring}$ .

In accordance with these statements, Figs. 16, 17, 18 and 19 propose the energy terms respectively stored by the glass panels, the cables and the dissipative devices.

Interesting structural benefits are strictly connected to the sliding of the friction apparatus, although the elastic component of the device involves an additional improvement in the energetic balance of the moving façade.

Fig. 16 refers, in particular, to the façade-module not equipped by dissipative devices, whereas Figs. 17, 18 and 19 display the energetic contributions associated to the façade-module equipped by a single vertical device. The sliding force was assumed equal to  $F_{y,D} = 750\text{kN} \cong 2.5H_0$ , whereas the elastic stiffness of the device was set equal to  $k_D = \infty \cong 1000 k_{cable}$  (Fig. 17),  $k_D = 5k_{cable}$  (Fig. 18) and  $k_D = k_{cable}$  (Fig. 19) respectively.

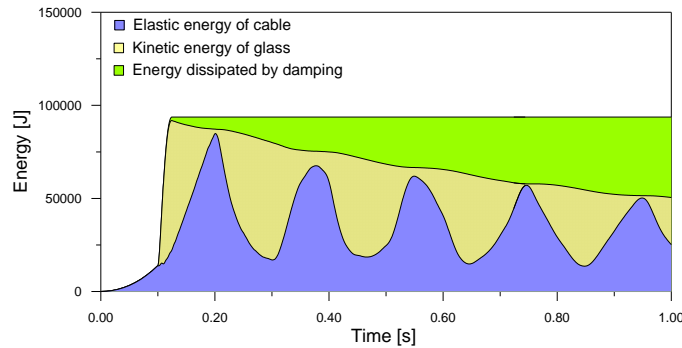


Fig. 16 Energy dissipation of the façade not equipped by dissipative devices, as a function of time

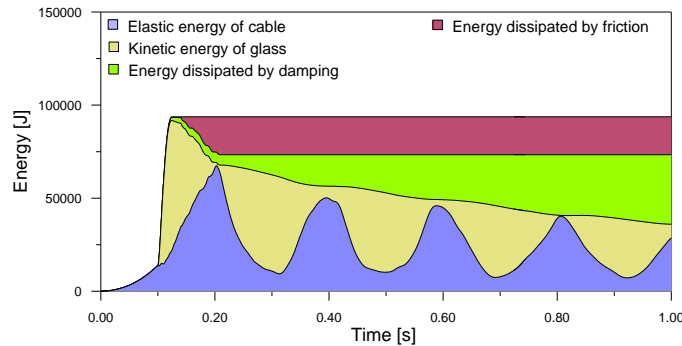


Fig. 17 Energy dissipation of the façade equipped by dissipative devices, as a function of time (single vertical device,  $F_{y,D} \cong 2.0H_0$  and  $k_D = \infty$ )

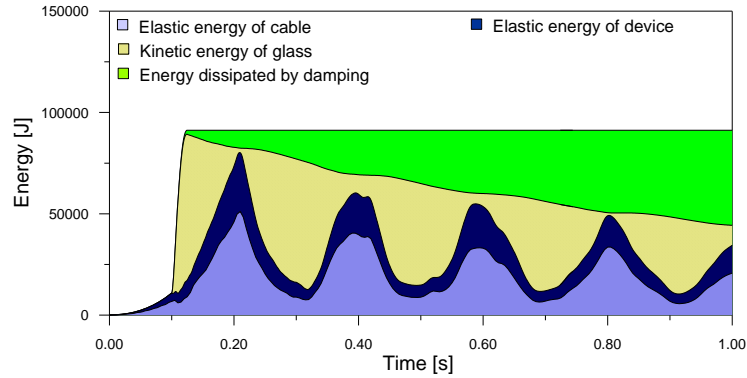


Fig. 18 Energy dissipation of the façade equipped by dissipative devices, as a function of time (single vertical device,  $F_{y,D} \cong 2.0H_0$  and  $k_D = k_{cable}$ )

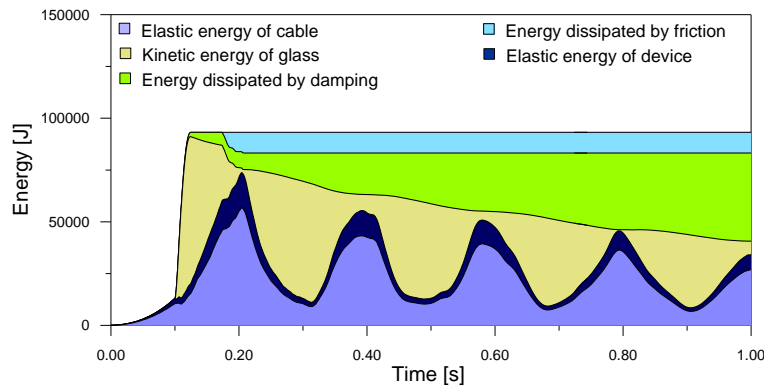


Fig. 19 Energy dissipation of the façade equipped by dissipative devices, as a function of time (single vertical device,  $F_{y,D} \cong 2.0H_0$  and  $k_D = 5k_{cable}$ )

When the façade-module is not equipped by devices (Fig. 16), the instant in which the increment of elastic energy in the cables  $\Delta E_{cables}$  attains its maximum value ( $t \cong 0.20s$ ) is typically characterized by a minimum increment of kinetic energy  $\Delta E_{glass}$  in the laminated glass sheets. This aspect cannot be ignored in the design of the bearing components of the façade, just because the increase of tensile stresses in the cables is strictly depend on the amount of energy  $\Delta E_{cables}$ .

The efficacy of the proposed dissipative system can be partly noticed from Fig. 17, where the term  $\Delta E_{cables}$  is strongly reduced – compared to Fig. 16 - due to the adopted devices. Contrarily, in the same figure it can be noticed that the elastic spring constituting the device does not offer any contribution in the definition of the energetic equilibrium of the façade-module, since the devices are assumed to behave rigid-plastically.

Because of this reason, with specific attention for the glass panels, the increment of kinetic energy  $\Delta E_{glass}$  is not affected by the presence of the dissipative devices (Fig. 17,  $t \cong 0.20s$ ), especially in the initial instants, but significant benefits can be clearly appreciated only in the subsequent instants of the investigated dynamic response.

In Fig. 18 an opposite design condition is proposed. The friction mechanism constituting the device does not dissipate part of the blast-induced energy, since the device is not sufficiently rigid and it does not plasticize after the explosion has been occurred. This limit condition should

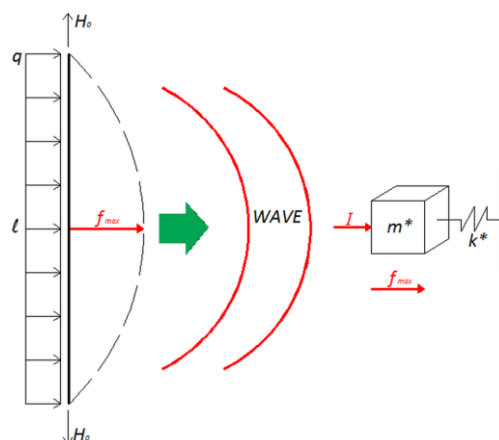


Fig. 20 Static and dynamic approach for a preliminary estimation of blast-induced effects on single-way cable-supported façades

undoubtedly be avoided, since the potentiality of the proposed devices is not exploited at best.

Finally, in Fig. 19 the optimal energetic condition for the examined case study is proposed. In it, both the friction mechanism and the elastic component of the device are opportunely calibrated, therefore the main components of the façade are strongly mitigated.

## 6. Analytical estimation of the blast-induced effects

A simple and rational estimation of the façade blast-induced response does not necessarily requires the use of advanced FE-numerical simulations. The analytical procedure proposed in this section, for example, summarizes the examined multi-degree-of-freedom (MDOF) cable-supported façade with an equivalent single-degree-of-freedom (SDOF) one.

Analyzing the behavior of the façade from an energetic point of view, it is possible to observe that when invested by the blast pressure the structure bends and, reaching the maximum deformed configuration, it partly returns the stored energy in the form of elastic energy to the bearing cables. In this manner, the laminated glass panels are pushed back toward their initial position by means of an oscillatory damped form of motion.

The blast-invested cable-supported façade approximately behaves as a SDOF that receives an external total impulse  $I$ . Initially the laminated glass panels acquire a quantity of motion  $Q = I = M\dot{v}$  and the system starts to oscillate with an initial velocity  $\dot{v}$ , having defined  $M=1470$  kg the total mass of the moving facade-module.

### 6.1 Dynamic parameters of the SDOF-system

The essential dynamic parameters of the equivalent SDOF-system can be estimated, referring to Ritz's method, by using the classical energetic approach. In these hypotheses, the original dynamic problem is statically solved and the single pretensioned cable constituting the studied façade-module is considered subjected to a uniformly distributed blast load  $q_{blast}$ , representative of the instantaneous blast wave pressure affecting the façade (Fig. 20). For this purpose, the length

$l_{cable}$  of the cable and the amount of the pretension force  $H$  affecting it should be taken into account.

Before the explosion occurs, the total pretension in the cable is  $H=H_0$ .

Considering the pretensioned cable having uniform properties along its length, its free vibration equation of motion is

$$H \frac{\partial^2 v(x,t)}{\partial x^2} = \mu A_{cable} \frac{\partial^2 v(x,t)}{\partial t^2} \quad (6)$$

with  $\mu$  the mass density per unit of length of the glass system;  $A_{cable}$  the cross-section area of the cable;  $v(x,t)$  the transversal displacement of the generic section. To approximate the motion of the cable system with a SDOF one, it is necessary to assume that the cable could deform only in a single shape (e.g., a parabolic shape).

In this context, the elastic and the kinetic energies of the cable system are respectively defined as:

$$E_{elastic}^{cable} = \frac{1}{2} \int_0^{l_{cable}} H v' dx \quad (7a)$$

$$E_{kinetic}^{cable} = \frac{1}{2} \int_0^{l_{cable}} \mu A_{cable} \dot{v}^2 dx \quad (7b)$$

On the other hand, the maximum elastic and the kinetic energies of a SDOF system in undamped free vibrations are commonly expressed as

$$E_{elastic}^{SDOF} = \frac{1}{2} k^* u_{max}^2 \quad (8a)$$

$$E_{kinetic}^{SDOF} = \frac{1}{2} m^* \dot{u}_{max}^2 \quad (8b)$$

with  $u_{max}$  and  $\dot{u}_{max}$  its maximum displacement and velocity, respectively.

The equivalent mass  $m^*$  and the equivalent stiffness  $k^*$  can be estimated by equaling both the elastic (Eqs. (7a) and (8a)) and the kinetic (Eqs. (7b) and (8b)) energies of the cable system and the SDOF one, thus hence resulting

$$m^* = \frac{16M}{30} \quad (9)$$

$$k^* = \frac{16H}{3l_{cable}} \quad (10)$$

being the fundamental period of vibration given by

$$T_0^* = 2\pi \sqrt{\frac{m^*}{k^*}} = 2\pi \sqrt{\frac{M l_{cable}}{10 H}} \quad (11)$$

It should be noticed, in this context, that Eq.(11) does not take into account the axial deformability of the cable. Due to the nature of explosive events, typically characterized by notable intensity and extremely short duration, it is evident that these assumptions do not involve

excessive errors or extreme simplifications in a first assessment of the façade dynamic response.

### 6.2 Estimation of the blast-induced dynamic response

Neglecting possible damping contributions, due to the energy conservation, once the explosion has been occurred the kinetic and the strain energies must equal to the incoming blast-energy

$$\frac{1}{2} m^* \dot{u}^2 + \frac{1}{2} k^* u^2 = E_{blast} \quad (12)$$

In Eq. (12),  $u$  and  $\dot{u}$  respectively denote the displacement and the velocity attained by the oscillating SDOF system due to the explosion;  $m^*$  and  $k^*$  were defined by Eqs. (9) and (10), while  $E_{blast} = I^2/2M$  is representative of the blast-induced energy.

Impulsive loads, such as explosions, are generally characterized by relatively short duration. Damping has scarce importance in controlling the dynamic response of the blast-invested structure and the maximum effects of the applied impulsive loads are attained in a very short time ( $\approx 0.02s$ ), before damping contributions could manifest.

In these hypotheses, Eq. (12) can be considered as the equation able to governs the blast-response of the equivalent SDOF system. In its maximum deformed configuration - typically characterized by maximum potential energy and kinetic energy equal to zero - the maximum displacement attained by the SDOF system due to the explosion results

$$u_{max} = \sqrt{\frac{I^2}{M k^*}} = I \sqrt{\frac{16}{30 m^* k^*}} \quad (13)$$

Similarly, when the potential energy vanishes and the kinetic energy is maximum, the velocity induced by the explosive event can be estimated as

$$\dot{u}_{max} = \sqrt{\frac{I^2}{M m^*}} = \frac{I}{m^*} \sqrt{\frac{16}{30}} \quad (14)$$

### 6.3 Iterative procedure

An accurate evaluation of the equivalent stiffness  $k^*$  (Eq. (10)) - and therefore of the maximum displacement due to the design blast load (Eq. (13)) - should be carried-out by taking into account that the initial pretension force  $H_0$  affecting the cables abruptly increases, due to the explosive event.

Assuming for each deformed cable a parabolic shape function, the increase  $H_{blast}$  of the initial pretension  $H_0$  is

$$H_{blast} = \frac{8 E_{cable} A_{cable} u_{max}^2}{3 l_{cable}^2} \quad (15)$$

with  $E_{cable}$  the Young's modulus of steel and  $u_{max}$  given by Eq. (13).

Based on Eq. (15), the total pretension force affecting the cable after the explosion is consequently given by

Table 2 Numerical and the analytical estimation of maximum blast-induced effects on the studied façade-module

	ABAQUS Positive phase	ABAQUS Positive and negative phases	Analytical model
Fundamental period $T_0$ [s]	0.51	0.51	0.53 (Eq. (11))
Maximum displacement $u_{\max}$ [m]	0.90	0.60	1.00 (Eq. (13))
Maximum velocity $\dot{u}_{\max}$ [m/s]	15.00	17.20	15.90 (Eq. (14))
Maximum pretension in the cable $H_{\max}$ [kN]	1190	913	940 (Eq. (16))

$$H = H_{\max} = H_0 + H_{blast} \quad (16)$$

In this context, it is clear that to properly estimate  $u_{\max}$  an iterative process should be performed by replacing Eq. (16) in Eq. (10), until the obtained value  $u_{\max}$  (Eq. (13)) remains constant.

As shown in Table 2, the comparison between the numerical and the analytical results obtained for the examined façade-module under Level D blast loads generally highlighted a rather appreciable agreement between them, hence suggesting the accuracy and validity of the simplified SDOF procedure.

## 7. Conclusions

In the paper, the behavior of a cable-supported façade subjected to high-level blast wave pressures has been numerically and analytically investigated. An innovative and efficient system able to dissipate part of the blast-induced stresses exerted against the examined curtain wall was presented.

At first, an accurate FE model was developed, in order to describe accurately the nonlinear dynamic behavior of the examined façade. Numerical results obtained from preliminary nonlinear dynamic analyses generally highlighted that the global behavior of the façade is essentially governed by the pretensioned cables. At the same time, the glass panels, typically characterized by brittle elastic behavior, are subjected to high peaks of tensile stresses that could compromise the integrity of the cladding wall.

In these hypotheses, in order to mitigate as much as possible the blast-induced stresses on the structural damages, an additional dissipative system was proposed to be installed at the ends of the bearing cables. Three different technological solutions were considered, respectively characterized by the introduction of (i) a single vertical device at the top of each cable, or two devices (ii) vertically or (iii) horizontally oriented, respectively) at both the cables ends. The first solution (i) generally appeared more convenient than the others, not only from a purely structural point of view, but also in energetic and economic terms. The performed analyses manifested an appreciable protective function of the proposed devices, since they clearly provide a marked decrease of maximum tensile stresses in the cables, without involving noteworthy increase of the corresponding maximum deflections. As a result, the proposed devices allow to preserve the critical components of the glass-steel system, hence improving the reliability of the façade and minimizing possible injured occupants.

In conclusion, an analytical model based on energetic considerations was also presented. The simplified analytical formulations, based on SDOF assumptions, generally provided predictions well agreeing with numerical estimations obtained from advanced FE simulations, hence suggesting their accuracy for rational estimation of maximum effects of blast events on cable-supported façades.

## References

- Baker, W.E., Cox, P.A., Wsetine, P.S., Kulesz, J.J. and Strehlow, R.A. (1983), *Explosion Hazards and Evaluation*, Elsevier Scientific Publishing Company, New York.
- Bulson P.S. (1997), *Explosive Loading of Engineering Structures*, E & FN Spon, Chapman & Hall, London.
- Corely, W.G., Mlarkar, P.F., Sozen, M.A. and Thornton, C.H. (1998), "The Oklahoma city bombing: summary and recommendations for multihazard mitigation", *J. Perform. Constr. Facil.*, ASCE, **12**(3), 100-112.
- Dassault Systèmes Simulia Corp. (2009), "ABAQUS ver. 6.9 User's Manual", Providence, RI, USA.
- Feng, R.Q., Zhang, L.L., Wu, Y. and Shen, S.Z. (2009), "Dynamic performance of cable net facades", *J. Construct. Steel Res.*, **65**, 2217-2227.
- GSA-TSO1-2003 (2003), "Standard test method for glazing and window systems subject to dynamic overpressure loadings", U.S. General Service Administration.
- Lam, N., Mendis, P. and Ngo, T. (2004), "Response spectrum solutions for blast loading", *Elec. J. Struct. Eng.*, **4**, 28-44.
- Li, Q.S. and Li, Q.G. (2005), "Time-dependent reliability analysis of glass cladding under wind action", *Struct. Eng.*, **25**(11), 1599-1612.
- Mays, G.C. and Smith, P.D. (1995), *Blast Effects on Buildings*, Thomas Telford Ltd.
- Norville, H.S. and Conrath, E.J. (2001), "Considerations for blast-resistant glazing design", *J. Arch. Eng.*, ASCE, **7**, (3), 80-86.
- Schlaich, J., Schober, H. and Moschner, T. (2005), "Prestressed cable net facades", *Struct. Eng.*, **15**(1), 36-9.
- Schmidt, J.A. (2003), "Structural design for external terrorist bomb attacks", *Struct.*, **3**, 21-23.
- Smith, D. (2001), "Glazing for injury alleviation under blast loading - United Kingdom practice", *Proceedings of the seventh international conference on architectural and automotive glass*, Glass Processing Days, Tamglass Ltd. Tampere.
- TM 5-1300 (1990), "The design of structures to resist the effects of accidental explosions", U.S. Departments of the Army, the Navy and the Air Force, Technical Manual, Washington DC.
- Weggel, D.C., Zapata, B.J. and Kiefer, M.J. (2007), "Properties and dynamic behavior of glass curtain walls with split screw spline mullions", *J. Struct. Eng.*, ASCE, **133**(10), 1415-1425.